UNIVERSITÀ DI PADOVA
Dipartimento
di Geoscienze

INGV

New constraints on Vp/Vs ratios and stress distribution at Etna volcano from anisotropic joint P- and S-wave tomography

Kira van Helden*, Brandon Vanderbeek***, Gianmarco Del Piccolo*, Manuele Faccenda*, Rosalia Lo Bue**, Elisabetta Giampiccolo**, Ornella Cocina**, and Marco Firetto Carlino**

**Università degli studi di Padova, Dipartimento di Geoscienze, Padova, Italy; **Istituto Nazionale di Geofisica e Vulcanologia, Osservatorio Etneo, Catania, Italy; ***University of Oxford, Department of Earth Sciences, Oxford, United Kingdom*

PROBABILISTIC TOMOGRAPHY: UNCERTAINTY OF VP/VS ANOMALIES

Despite (or perhaps because of) being one of the most extensively studied volcanoes in the world, the wide variety of tomographic models[1,3,4,6,8,10,12] published of Etna volcano (Sicily, Italy) show only limited agreement. Particularly little agreement can be found between recovered Vp/Vs ratios, an important parameter for identifying rock fluid properties. Since S-waves are generally noisier, have ray-orthogonal particle motion, and exhibit splitting in the presence of anisotropy, high quality S-wave arrival time observations are much more scarce than P-wave observations. Additionally, most common deterministic imaging methods are limited by the underdetermination of the inverse problem, and rely on damping and smoothing constraints to find a unique solution; a problem that is exacerbated by poor S-wave ray coverage. We address this issue by applying probabilistic tomography[4,5] (transdimensional Bayesian Monte Carlo sampling), allowing for robust uncertainty estimation (see methods, Fig. 8-9).

CRUSTAL ANISOTROPY DUE TO FLUID-FILLED FRACTURES

The preferential alignment of eruptive fissures, dikes, sills, and (fluid-filled) microcracks with the local stress field - typical for the crust beneath volcanoes - causes the velocity of seismic waves to vary with propagation direction with respect to these aligned fractures (seismic anisotropy). Previous studies[4,8,9] have demonstrated the presence of strong crustal anisotropy beneath Mt. Etna. Being an indicator of rock fluids, the Vp/Vs ratio is inherently linked to seismic anisotropy due to aligned fluid-filled fractures. Therefore, joint P- and S-wave tomography has the potential to reveal the connection between stress state (orientation and magnitude of anisotropy) and rock fluid properties (directionally invariant Vp/Vs ratio). **Here we show both purely isotropic (Fig. 1-2) and anisotropic (Fig. 3-6) inversion results, highlighting the similarities and differences in recovered Vp/Vs ratios.**

MT. ETNA'S SUBSURFACE STRUCTURE - PREVIOUS vs NEW RESULTS

Many studies have identified a high Vp body (HVB) at shallow depth below the volcano's summit, indicating a solidified magma body. However, at deeper depths, findings start to vary more. More recent anisotropic tomography studies[4,8] have identified a low Vp body (LVB) extending roughly between 6 and 16 km depth b.s.l., coinciding with a spherical pattern of anisotropic symmetry axes. A likely interpretation would be the presence of a magma storage zone existing of a radial pattern of dikes. Our joint P- and S-wave tomography recovers both the shallow HVB and deeper LVB found in previous studies, as well as the spherical pattern of anisotropic axes. Since Vp/Vs generally increases with melt content, we would expect a high Vp/Vs ratio at the location of the LVB. However, we observe a region of low Vp/Vs. Potential causes for a decreased Vp/Vs include: (1) the presence of exsolved gas[7,14], (2) wide/spherical cracks[11], and (3) artifacts of anisotropy that might not be properly accounted for in the inversion due to bad S-wave ray coverage and/or faulty polarization measurements (see next paragraph).

CRUSTAL ANISOTROPIC S-WAVE TOMOGRAPHY: REMAINING CHALLENGES

Our method for anisotropic S-wave tomography was developed for teleseismic imaging of the mantle[13]. As shown by this poster, the method has strong potential for local earthquake crustal imaging of volcanic settings as well. However, it introduces some specific challenges: **(1)** Anisotropic S-wave tomography requires the measurement of principle polarization directions. In contrast to teleseismic events, waveform recordings of a local earthquake cannot simply be stacked to suppress noise. Computing a polarization angle of single waveforms (or small stacks of similar events) increases the need for high quality waveform data. This results in the extremely uneven coverage of 8,457 S- and 39,500 P-rays. Unsurprisingly, we obtain a very smooth Vp/Vs model, which might not adequately reflect true anomalies. We aim to keep improving our signal processing workflow in order to increase the S-wave ray coverage. **(2)** To obtain sufficient resolution on a crustal scale, we need to work with higher frequency data. However, our approximation of anisotropy requires the waveform period to be sufficiently long w.r.t. the split time ($T / | t'' - t' | > 5$). Splitting measurements will be incorporated in our workflow, so that measurements that do not meet this criterion can receive a smaller weight in the inversions.



References:

ISOTROPIC RESULTS

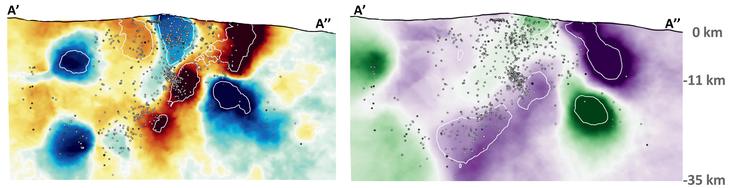


Fig 1. Purely isotropic inversion results. Vertical cross sections NW-SE of isotropic (left) Vp and (right) Vp/Vs anomalies with respect to the 1D reference model. Regions with RSD = std. dev. / mean < 1 are outlined white. Events colored by number of P vs S observations.

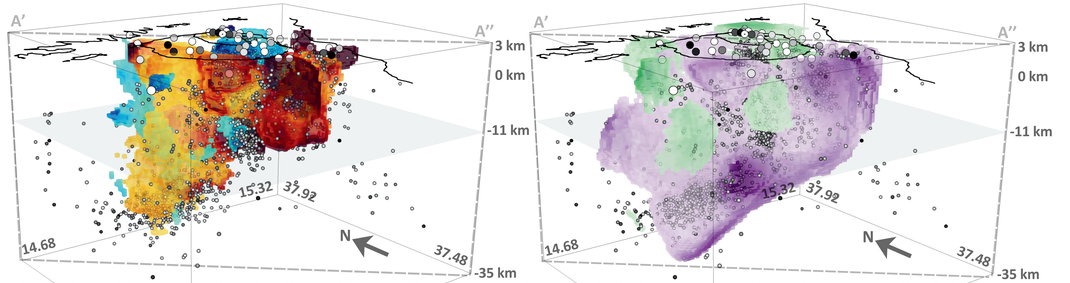


Fig 2. Purely isotropic inversion results. 3D overview of isotropic (left) Vp and (right) Vp/Vs anomalies with respect to the 1D reference model. Only > 2% anomalies are shown with 68% hdi < 0.1 (see methods, fig. 9). Events (small spheres) and stations (outlined circles) colored by number of P vs S observations.

ANISOTROPIC RESULTS

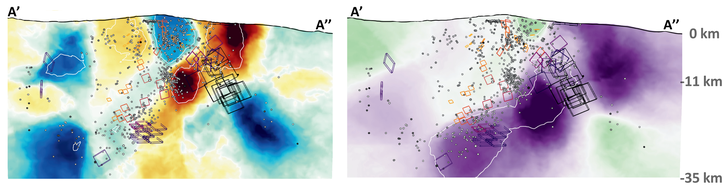


Fig 3. Anisotropic inversion results. Vertical cross sections NW-SE of directionally invariant (left) Vp and (right) Vp/Vs anomalies with respect to the 1D reference model. Fast propagation planes (orthogonal to anisotropic symmetry axis) are colored and scaled by magnitude. Regions with RSD = std. dev. / mean < 1 are outlined white. Events colored by number of P vs S observations.

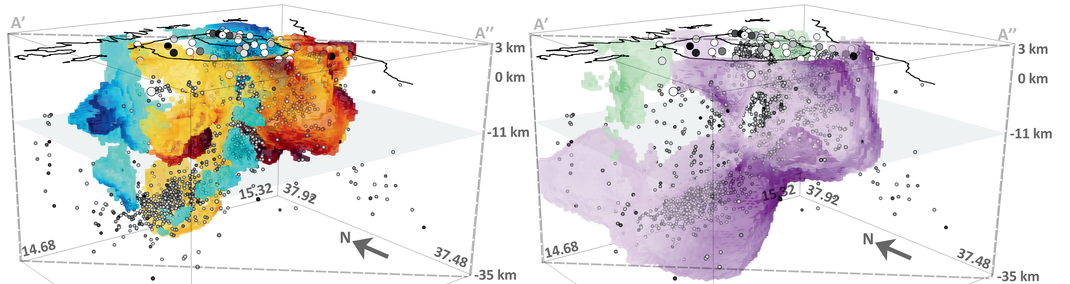


Fig 4. Anisotropic inversion results. 3D overview of directionally invariant (left) Vp and (right) Vp/Vs anomalies with respect to the 1D reference model. Only > 2% anomalies are shown with 68% hdi < 0.1 (see methods, fig. 9). Events (small spheres) and stations (outlined circles) colored by number of P vs S observations.

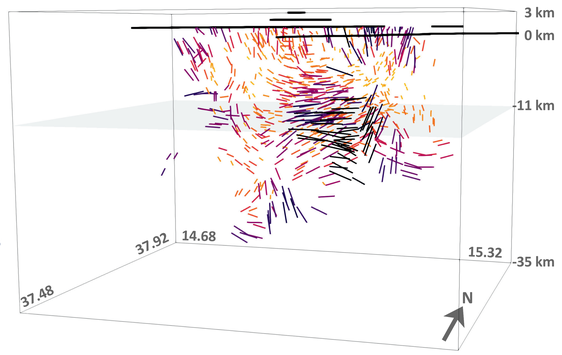


Fig 5. Anisotropic inversion results. 3D overview of anisotropic symmetry axes. Only axes with a directional bias > 75% (meaning 75% agreement in direction) are shown, and the axes are colored and scaled by magnitude.

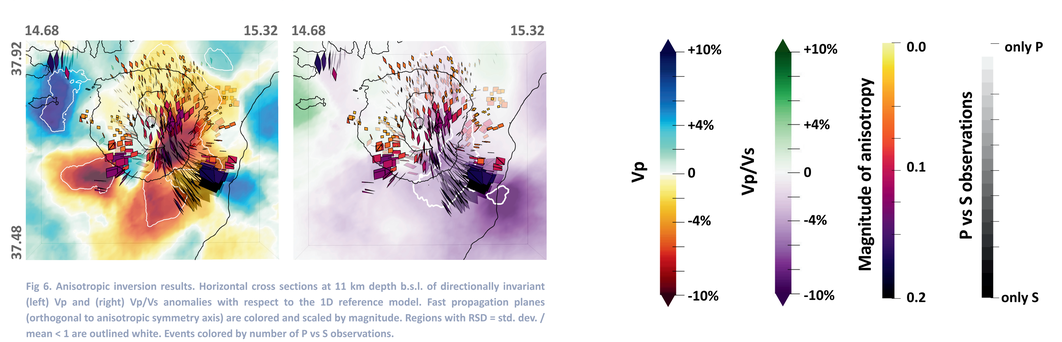


Fig 6. Anisotropic inversion results. Horizontal cross sections at 11 km depth b.s.l. of directionally invariant (left) Vp and (right) Vp/Vs anomalies with respect to the 1D reference model. Fast propagation planes (orthogonal to anisotropic symmetry axis) are colored and scaled by magnitude. Regions with RSD = std. dev. / mean < 1 are outlined white. Events colored by number of P vs S observations.

METHODS

PRINCIPLE POLARIZATION DIRECTION[13]

- For each station, events are clustered by location and waveform similarity
- Q and T components are concatenated and aligned using multi-channel cross correlation methods[2] (Fig. 7A)
- Eigen decomposition of the covariance matrix of the Q and T traces yields the principle polarization direction (Fig. 7B)
- The polarization is measured for both individual traces and stacks of similar waveforms → result with largest energy reduction on the transverse (x2) component is selected (Fig. 7C)

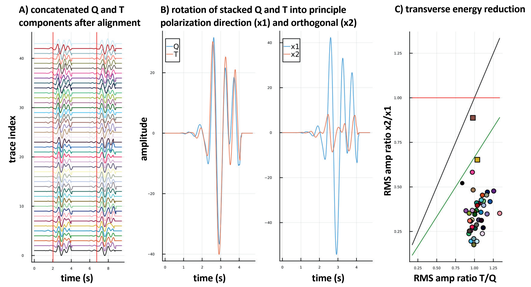


Fig 7. Example of a high quality polarization angle measurement. See text for methods.

TRANSDIMENSIONAL BAYESIAN MARKOV CHAIN MONTE CARLO SAMPLING[4,5]

- This probabilistic method takes a starting velocity model (either random or in the case of this study, a 1D reference model) and proposes random perturbations to this model.
- This random perturbation can be a perturbation to a model parameter, but it can also be the addition or rejection of a cell, making the model resolution an inversion parameter itself.
- Each perturbed model is accepted or rejected based on the data fit.
- We run 24 independent Markov chains with 6e5 iterations.
- The final model is the mean of all accepted models in all chains.
- Each gridpoint has its own posterior distribution for each model parameter (Fig. 9) → we use the high density interval and standard deviation relative to the mean (RSD<1) as a measure for model robustness.

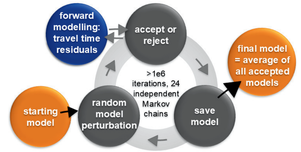


Fig 8. Flowchart of probabilistic imaging method.

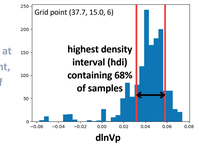


Fig 9. Posterior distribution of dlnVp at an example grid point, showing definition of the highest density interval (hdi).

CONCLUSIONS & FUTURE WORK

- **Our results confirm the shallow HVB found by previous studies. The LVB with a radial pattern of fast propagation planes is found as well, but unexpectedly overlaps with a region of low Vp/Vs. The origin of this low Vp/Vs volume is still up for debate.**
- **The purely isotropic and anisotropic inversions yield similar velocity anomalies. However, the anisotropic result fits the P-wave data much better, but the S-wave data slightly worse.**
- **Future work will therefore focus on improving polarization angle measurements and increasing S-wave ray coverage.**